Eur. Phys. J. Appl. Phys. **55**, 20501 (2011)
DOI: 10.1051/epjap/2011100296

THE EUROPEAN PHYSICAL JOURNAL
APPLIED PHYSICS

Regular Article

Photon-induced tunable and reversible wettability of pulsed laser deposited W-doped ZnO nanorods

B.D. Ngom[1,2,a], O. Sakho[1], S. Ndiaye[1], R. Bartali[3], A. Diallo[1], M.B. Gaye[1], S. Bady[1], N. Manyala[4], M. Maaza[2], and A.C. Beye[1]

[1] Groupes de Physique du Solide et Sciences des Matériaux (GPSSM), Faculté des sciences et Techniques, Université Cheikh Anta Diop de Dakar (UCAD), B.P. 25114, Dakar-Fann, Dakar, Senegal
[2] NANO-Sciences Laboratories, Materials Research Department, iThemba LABS, National Research Foundation, South Africa
[3] Fondazione Bruno Kessler – Centro Materiali e Microsistemi, Plasma and Advanced Material, Bio-MEMS, Via Sommarive 18, 38050 Povo, Trento, Italy
[4] Department of Physics, Institute of Applied Materials, University of Pretoria, Pretoria 0002, South Africa

Received: 20 July 2010 / Received in final form: 6 October 2010 / Accepted: 24 March 2011
Published online: 11 August 2011 –

Abstract. ZnO nanorods arrays were prepared on soda lime glass substrate by pulsed laser deposition method. Hexagonal rod-like ZnO rods were obtained under different conditions. Well-defined ZnO nanorods arrays were selected among different samples having various morphologies and sizes already studied by X-ray diffraction (XRD) and atomic force microscopy (AFM). Here, we report on the contact angle measurement (CAM) of one of these samples. A systematic change of the surface wettability is observed in W-doped ZnO nanostructures. The water contact angle (WCA) of a 1 wt.% of WO_3 target content was found to be the transition doping level from hydrophilic surface to a hydrophobic surface. We attributed the transition in surface wettability of the film with the doping to incorporation increase of tungsten into the film. Such characteristic surface wettability can play a key role in the adhesion of various layers on W-ZnO nanorods arrays for optoelectronic device applications.

1 Introduction

Wettability is a defining property of the interface between liquids and solids. Controlling surface wettability is of vital importance for a wide range of biological, chemical, and electronic applications [1,2]. The wetting behaviors are mainly governed by two factors, surface geometrical structure and chemical composition [2]. Transparent conductive oxides (TCOs) have been intensively studied for their potential in optoelectronic applications, including for the manufacture of organic light-emitting diodes (OLEDs). It is well known that indium tin oxide (ITO) is the most popular TCO, because of its high conductivity and transparency [3].

However, its chemical instability, toxic nature and high cost, combined with the diffusion of indium into surrounding organic materials, have stimulated efforts to find an alternative [4]. Among these materials, one of the most promising candidates is doped ZnO which has sufficiently high conductivity and a transmittance of over 90% in the visible range, even in samples grown at room temperature [5].

Optimized ZnO based TCO films could replace ITO as an anode material in OLED applications. In comparison with ITO, ZnO films are more stable in reducing ambient circumstance, more readily available, and less expensive [6]. Because of these characteristics, ZnO is often used as an anode material in photoelectronic devices such as solar cells, flat panel displays and OLEDs [7–10].

Because the anode materials in an OLED are in contact with organic molecules, both their surface chemical properties and their morphology affect the adhesion and alignment of molecules on the surface [11]. Therefore, a microscopic understanding of wettability in solid surfaces is fundamentally interesting and practically valuable. Furthermore, the absorption of water on metal-oxide surfaces is an important subject in its own right, due to its crucial role in gas sensors, catalysis, photochemistry and electrochemistry. It is well known that the measurement of the water contact angle (WCA) could reveal much useful information about characteristics of surface nanostructure and morphology [12]. However, there have been few studies of the surface wettability of the transparent conducting oxide ZnO nanostructures.

Recently, with the development of smart devices, such as intelligent microfluidic switch, reversibly controlling the

[a] e-mail: ngom@emt.inrs.ca; bdngom@gmail.com

surface wettability has aroused great interest and can be realized by modifying the surface properties.

In this paper, controllable wettability of aligned W-doped ZnO nanorods films fabricated by pulse laser deposition is reported. These inorganic oxide films show hydrophobicity and hydrophilicity at different conditions, and the wettability can be reversibly switched by alternation of ultraviolet (UV) irradiation and dark storage. Such special wettability will greatly extend the applications of ZnO films to many other important fields ranging from biological, chemical, and electronic applications.

The unique self assembly of these nanostructures with tunable complexity presents a convenient and effective means to adjust the surface wetting behaviors. The dependence of the water contact angle of the grown films on the amount of W-doping was investigated.

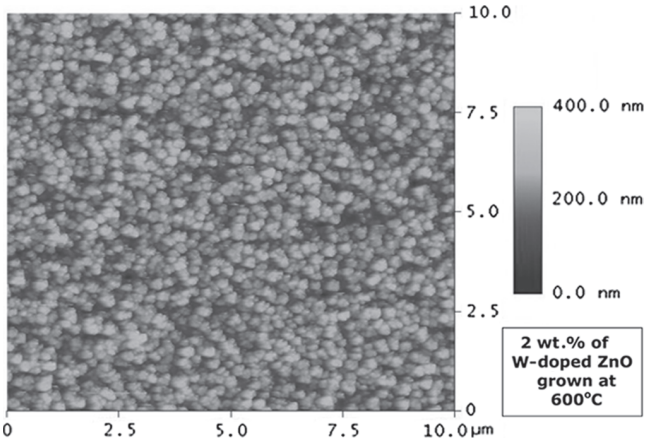

Fig. 1. (Color online) 2D AFM images of the W-doped ZnO nanorods deposited with 2 wt.% target composition.

2 Experimental details

Cylindrical pellets "$\phi \approx 15$ mm and about 2 mm thick" were used as targets prepared by standard sintering method from pure oxide metal powders "Johnsson Mathey, purity 99.8%" for WO_3 and "Alpha Aesar 99.999% purity" for ZnO. The detailed experimental conditions for the pulsed laser deposition growth, X-ray diffraction structural characterization of the samples are reported in our previous work [13]. However, the morphology was studied using an atomic force microscopy (AFM) model NanoMan V Veeco. The AFM images were analyzed with Nanoscope V700 software. The surface topography mappings were obtained in air subsequent to a special cleaning treatment before scanning. All images were obtained in direct tapping mode with standard Si tips of nominal radius 10–20 nm. Topography scanning on the nanostructures' surface was measured over scan range of 10×10 μm^2.

The contact angle measurements were carried out on the nanostructures by the sessile drop method. It consists of depositing a liquid drop on a solid surface and measuring the angle between the solid surface and the tangent to the drop profile at the drop edge. The volume of the drop was about 16 μl, the analysis software used was a drop analysis (image J) based on B-spline.

3 Results and discussion

The typical X-ray diffraction patterns for W-doped ZnO thin film grown from the 1 wt.% target were shown to exhibit two peaks: strong and a weak at (0 0 0 2) and (0 0 0 4) diffraction indices at angles of 34.41° and 72.75° respectively. Detailed information on the effect of W-doping on the structural properties of the ZnO is discussed in our previous work [13].

Moreover the AFM image of the undoped ZnO samples revealed nanorod morphology but dispersed all over the substrate and with lower surface roughness of about 10.2 ± 1.2 nm. Figure 1 shows that with W-doping, the nanorods are spontaneously organized into some ordered parallel structures with the major axis pointing perpendicularly to the substrate surface. The tungsten appears to play the role of a catalyst rather than a substitute of zinc; similar results have been reported for the growth of ZnO nanostructures where the Zn acted as a self catalyst for the orientation of the nanostructures as suggested by the results in the lattice parameter c [14].

The AFM images of the sample grown with 2 wt.%, the grain density decreases and the AFM image of the film shows well-oriented nanorods like, with an increase of the surface roughness to 33.1 ± 1.8 nm. The detailed influence of W-doping on the morphology of the ZnO is also discussed in our previous work [13].

The dependence of the water contact angle (WCA) on the different W-doping concentration of samples is shown in Figure 2. The inset to Figure 2 shows a water droplet on the film fabricated from the target containing 2 wt.% of WO_3 target composition. We obtained the WCA, which shows the wettability changes of the surface, by measuring the angle between the sample surface and the water-droplet boundary on the surface.

Because the wettability determines adhesion with neighboring layers that include organic materials in OLEDs, it is an important parameter in OLED device fabrication. As seen in Figure 2, the result shows the significant differences in surface wettability for different W concentrations.

Interestingly, the maximum and minimum WCA values for W-doped ZnO film at different WO_3 wt.% composition were found. At film grown with 0 wt.%, the WCA dropped from about 90° to 58° after the water droplet has been introduced on the film for 125 s as shown in Figure 3a.

We observed that the derivative of the WCA as a function of the time has a linear trend, as shown in Figure 3b, indicating an exponential decreasing of wettability.

As indicated by the following equations:

$$\frac{\partial \theta}{\partial t} = a - b\theta, \tag{1}$$

$$\theta = k + ce^{-b(t-t_i)}, \tag{2}$$

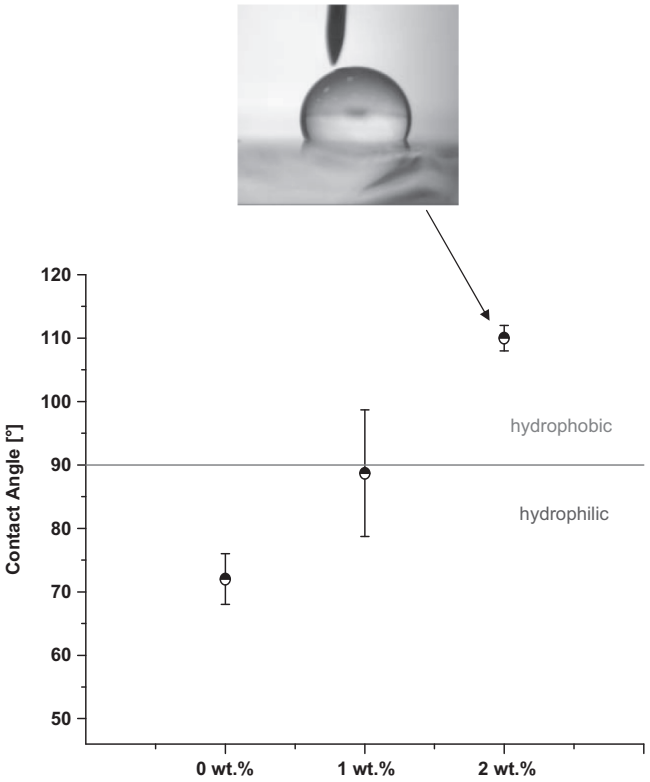

Fig. 2. (Color online) Water contact angle of the W-doped ZnO nanorods deposited with different target composition.

where θ is water contact angle, $k = a/b$ ratio and $c = \theta i - a/b$.

By equation (2) we can estimate the wettability at a time zero and the wettability at the steady state ($t =$ infinity). This indicates that the change of wettability is due to the increase in sensitivity of the water drop to the films during the time. When the time is zero the drop touches only the ZnO coating and we estimate that the intrinsic wettability of the coating is around 90°. For $t =$ infinity wettability reaches a precise steady state of 58°.

Knowing the wettability of substrate 42°, we can observe that the steady state is a composition of ZnO and glass wettability.

Applying the Cassie-Baxter equation for heterogeneous surface we can approximately estimate the surface wettability fraction due to the ZnO and that due to the glass:

$$\cos\theta_m = f_1 \cos\theta_1 - f_2 \cos\theta_2. \quad (3)$$

Imposing the following condition:

$$f_1 + f_2 = 1,$$
$$f_1 = 1 - f_2,$$

we can obtain $f_2 = -((\cos\theta_m - \cos\theta_1)/(\cos\theta_1 + \cos\theta_2))$, where θ_m = WCA measured at steady state (58°), θ_1 = contact angle of substrate (42°) and θ_2 = contact angle of ZnO (90°). In this case we estimate that the fraction of ZnO in the steady state is only 0.28 (∼30%). The fact the WCA is below 90° indicates a hydrophilic behavior of the film.

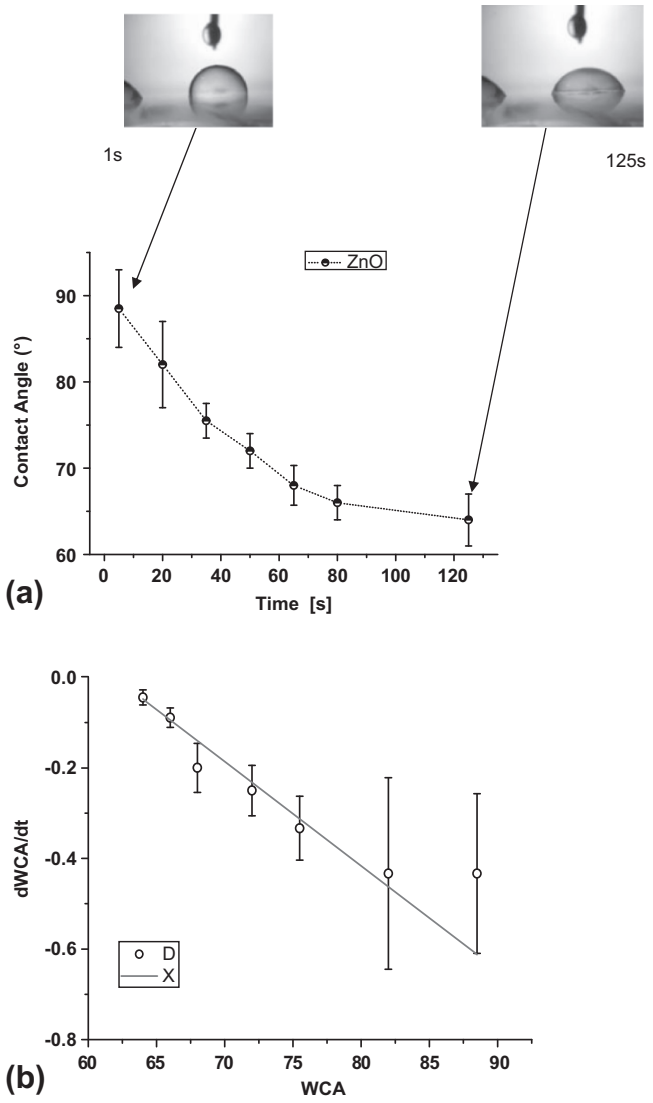

Fig. 3. (Color online) Time dependence of the water contact angle of the undoped ZnO nanorods.

The WCA increased with W concentration to a maximum of 110° for the sample prepared with 2 wt.% WO_3. This shows that the films are hydrophobic (110°), also in this case the wettability is due to the heterogeneity of the substrate but the complementary element of ZnO nanorods is the air that induces the hydrophobicity of the material. Therefore the hydrophobic behavior is related to the morphology of the substrate.

The hydrophobic behavior remains constant for the duration of the water droplet introduced on the surface of the sample as shown in Figure 4. The sample prepared with 1 wt.% of WO_3 shows the WCA of about 90° (see Fig. 2). This marks the wettability change from hydrophilic to hydrophobic with W concentration and hence could be regarded as the transition concentration between the two behaviors.

Upon UV (obtained from a 500 W Hg lamp with a filter centered at 365 nm) irradiation for 115 min on the sample prepared with 2 wt.% of WO_3 target composition,

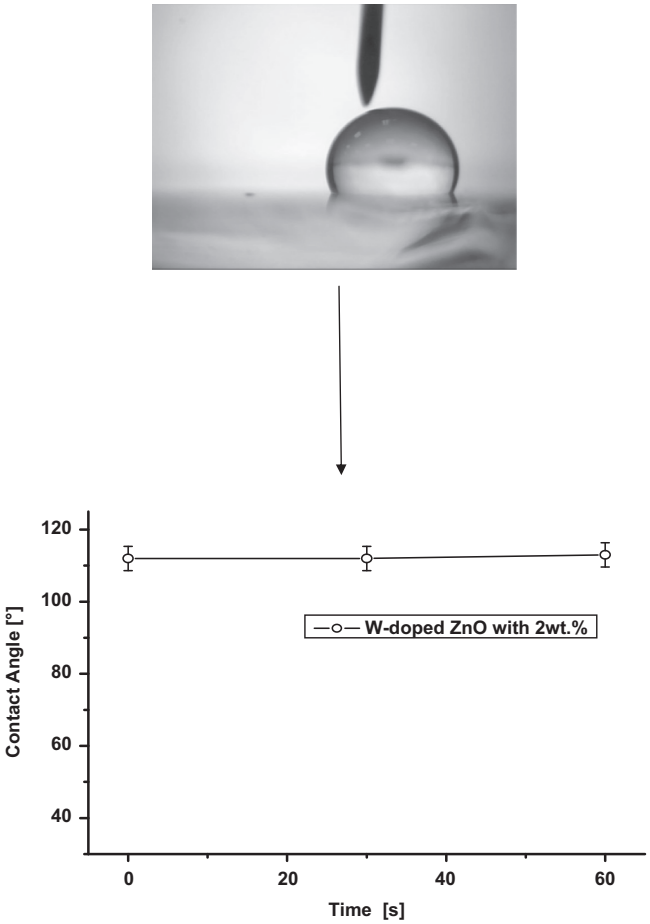

Fig. 4. (Color online) Time dependence of the water contact angle of the W-doped ZnO nanorods deposited with 2 wt.% target composition.

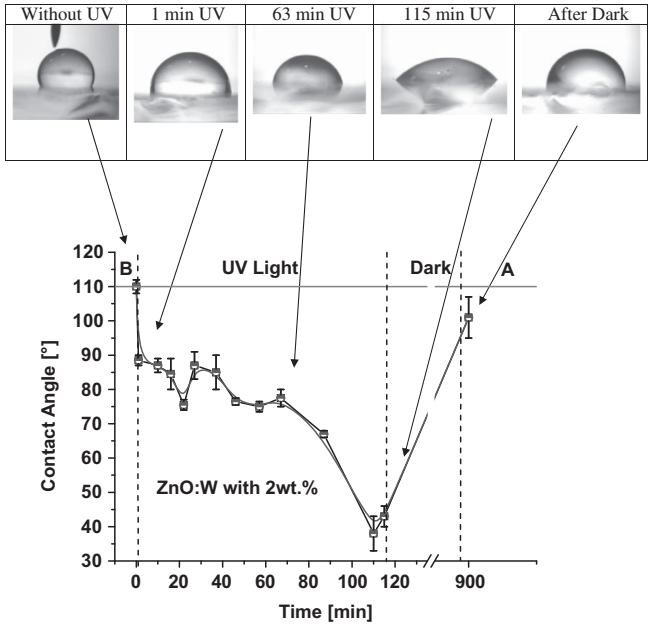

Fig. 5. (Color online) Effect of UV light and dark storage on the water contact angle of the W-doped ZnO nanorods deposited with 2 wt.% target composition.

the water droplet spread out on the film, resulting in a WCA of about 43° (Fig. 5). These results indicate that the wettability changes from a stable hydrophobicity to hydrophilicity. After the UV-irradiated films were placed in the dark, the hydrophobicity of the nanorods films was obtained again. This process has been repeated several times, and good reversibility of the surface wettability was observed.

But it is very interestingly observed that the WCA after 100 min reaches 40°, at exactly the same value of the substrate (42°). This indicates that the samples prepared with 0 wt.% of WO_3 are completely hydrophilic and the wetting of the surface is governed only by the substrate.

To thoroughly understand the reversible stable hydrophobicity to hydrophilicity transition of the aligned W-doped ZnO nanorod films, the surface free energy and the surface roughness, which are two main factors governing the surface wettability, are considered. It is well known that only when the surface free energies of the various crystallographic planes differ significantly could an anisotropic nanorod growth be realized [15] and a fast growing plane generally tends to disappear leaving behind slower growing planes with lower surface energy. For the anisotropic ZnO nanorod, the velocities of crystal growth in different directions were reported to be $[-1\ 0\ 0] > [-1\ 0\ 1] > [0\ 0\ 1] \approx [0\ 0\ -1]$ [16]. Figure 1 shows that the ZnO nanorods are highly vertically oriented with the well-faceted (0 0 1) end projecting out. Compared with other random orientation of ZnO nanocrystals films [17, 18], the as-prepared films have the lowest surface free energy. Figure 1 also shows that the nanorods grow separately on the substrate, and air can be present in the troughs between individual nanorods. The hydrophobicity of a rough surface can be intensified by increasing the proportion of air/water interface [19], for example, superhydrophobic surfaces have been successfully fabricated by the aligned carbon nanotubes and polymer nanofibers [20]. The nanorods and air composite rough surface structure in this case can also greatly enhance the hydrophobicity of the films. Accordingly, both the lower surface free energy and the higher surface roughness contribute to the hydrophobicity of the as-prepared films. As reported in reference [18], UV irradiation will generate electron-hole pairs in the ZnO surface, and some of the holes can react with lattice oxygen to form surface oxygen vacancies. Meanwhile, water and oxygen may compete to dissociate adsorption on the surface. The defective sites are kinetically more favorable for hydroxyl adsorption than oxygen adsorption. As a result, the surface hydrophilicity is improved, and the WCA of a relatively flat ZnO surface changes from 109° to 5° [18]. For a rough surface, water will enter and fill the grooves of the films, leaving only the up part of the nanorods not in contact with the liquid, which is the three-dimensional capillary effect of a rough surface [21]. This effect results in a hydrophilic surface. For instance, combining with the rough structure, the UV irradiation causes the surface wettability of aligned ZnO nanorods films to change from

stable hydrophobicity to hydrophilicity. It has been demonstrated that the surface becomes energetically unstable after the hydroxyl adsorption, while the oxygen adsorption is thermodynamically favored, and it is more strongly bonded on the defect sites than the hydroxyl group [18]. A similar result has also been observed on the TiO_2 surface [22,23]. Therefore, the hydroxyl groups adsorbed on the defective sites can be replaced gradually by oxygen atoms when the UV-irradiated films were placed in the dark. Subsequently, the surface evolves back to its original state (before UV irradiation), and the wettability is reconverted from hydrophilicity to hydrophobicity.

On the basis of the above analysis, it can be concluded that the reversible switching between hydrophilicity and stable hydrophobicity is related to the cooperation of the surface chemical composition and the surface roughness. The former provides a photosensitive surface, which can be switched between hydrophilicity and hydrophobicity, and the latter further enhances these properties. In addition, the reversible conversions of the surface wettability proceed only by the adsorption and desorption of surface hydroxyl groups at the outmost layer of oxide films [22], while the structure below the outmost layer remains stable, free from changes in chemical conditions. Therefore, it is reasonable that the reversible wettability switching properties of the as-prepared films exhibit long-term durability.

4 Conclusion

In summary, the wettability of aligned ZnO nanorod films was investigated. Reversible stable hydrophobicity to hydrophilicity transition was observed and intelligently controlled by alternation of UV illumination and dark storage. This reversible transition of surface wettability is a completely new concept for preparing smart films. This strategy can be extended to other stimuli-responsive surfaces with similar nanostructure and higher stability, which is certainly significant for future industrial applications.

We are thankful for financial support from the African Laser Centre (ALC) and the Nanoscience African Networkb (NANOAFNET) and also to iThemba LABS, a facility of the National Research Foundation and the CSIR-NLC of South Africa for the use of their facilities.

References

1. H. Gau, S. Herminghaus, P. Lenz, R. Lipowsky, Science **283**, 46 (1999)
2. X.J. Feng, L. Jiang, Adv. Mater. (Weinheim, Ger.) **18**, 3063 (2006)
3. H. Kim, C.M. Gilmore, A. Pique, J.S. Horwitz, H. Mattoussi, H. Murata, Z.H. Kafari, D.B. Chrisey, J. Appl. Phys. **86**, 6451 (1996)
4. H. Kim, C.M. Gilmore, J.S. Horwitz, A. Pique, H. Murata, G.P. Kushto, R. Schlaf, Z.H. Kafafi, D.B. Chrisey, Appl. Phys. Lett. **76**, 259 (2000)
5. M. Chen, Z.L. Pei, C. Sun, L.S. Wen, X. Wang, J. Cryst. Growth **220**, 254 (2000)
6. B. Szyszka, T. Höing, X. Jiang, A. Pflug, N. Malkomes, M. Vergöhl, V. Sittinger, U. Bringmann, G. Bräuer, in *Proc. of 44th SVC Technical Conference* (2001), p. 272
7. T.L. Yang, D.H. Zhang, J. Ma, H.L. Ma, Y. Chen, Thin Solid Films **326**, 60 (1998)
8. A.W. Ott, R.P.H. Chang, Mater. Chem. Phys. **58**, 132 (1999)
9. R.-C. Wang, C.-P. Liu, J.-L. Huang, S.-J. Chen, Appl. Phys. Lett. **88**, 023111 (2006)
10. Z.B. Deng, X.M. Ding, S.T. Lee, Appl. Phys. Lett. **74**, 2227 (1999)
11. Z.G. Guo, F. Zhou, J.C. Hao, W.M. Liu, J. Am. Chem. Soc. **126**, 15670 (2005)
12. T. Soeno, K. Inokuchi, S. Shiratori, Appl. Surf. Sci. **237**, 543 (2004)
13. B.D. Ngom, O. Sakho, N. Manyala, J.B. Kana, N. Mlungisi, L. Guerbous, A.Y. Fasasi, M. Maaza, A.C. Beye, Appl. Surf. Sci. **255**, 7314 (2009)
14. N. Wang, Y. Cai, R.Q. Zhang, Mater. Sci. Eng. R **60**, 1 (2008)
15. V.F. Puntes, K.M. Krishnan, A.P. Alivisatos, Science **291**, 2115 (2001)
16. L. Vayssieres, K. Keis, A. Hagfeldt, S.E. Lindquist, Chem. Mater. **13**, 4395 (2001)
17. M. Li, J. Zhai, H. Liu, Y.L. Song, L. Jiang, D.B. Zhu, J. Phys. Chem. B **107**, 9954 (2003)
18. R.D. Sun, A. Nakajima, A. Fujishima, T. Watanabe, K.J. Hashimoto, Phys. Chem. B **105**, 1984 (2001)
19. A.B.D. Cassie, S. Baxter, Trans. Faraday Soc. **40**, 546 (1944)
20. L. Feng, S.H. Li, Y.S. Li, H.J. Li, L.J. Zhang, J. Zhai, Y.L. Song, B.Q. Liu, L. Jiang, D.B. Zhu, Adv. Mater. **14**, 1857 (2002)
21. J. Bico, U. Thiele, D. Quere, Colloids Surf. A **206**, 41 (2002)
22. R. Wang, N. Sakai, A. Fujishima, T. Watanabe, K.J. Hashimoto, Phys. Chem. B **103**, 2188 (1999)
23. L.Q. Wang, D.R. Baer, M.H. Engelhard, A.N. Shultz, Surf. Sci. **344**, 237 (1995)